MR of Zellweger Syndrome

A. James Barkovich and Wallace W. Peck

PURPOSE: To determine characteristic MR imaging features of Zellweger syndrome. **METHODS:** Clinical records, laboratory records, and MR studies of six patients with Zellweger syndrome were reviewed retrospectively. MR studies were examined for the state of myelination; the presence, extent, and morphologic appearance of cerebral cortical anomalies; the status of the cerebellar cortex, basal nuclei, and brain stem; and the presence or absence of any regions of abnormal signal intensity. **RESULTS:** The diagnosis of Zellweger syndrome was established in all patients by clinical findings combined with laboratory and MR results. All patients had impaired myelination and diffusely abnormal cortical gyral patterns that consisted of regions of microgyria (primarily in the frontal and perisylvian cortex) together with regions of thickened pachygyric cortex (primarily perirolandic and occipital). The pachygyric regions were in the form of deep cortical infoldings. Germinolytic cysts were visible in the caudothalamic groove in all patients, seen best on coronal or sagittal T1-weighted images. One patient had T1 shortening in the bilateral globus pallidus, presumably related to hepatic dysfunction and hyperbilirubinemia. **CONCLUSION:** The combination of hypomyelination, cortical malformations that are most severe in the perisylvian and perirolandic regions, and germinolytic cysts are highly suggestive of Zellweger syndrome in the proper clinical setting.

Index terms: Brain, magnetic resonance; Children, diseases

AJNR Am J Neuroradiol 18:1163–1170, June 1997

Cerebrohepatorenal, or Zellweger, syndrome is a disorder of peroxisomal function that presents in the neonatal period with involvement of multiple organ systems. In this article, we share our experience in the magnetic resonance (MR) imaging of six patients with Zellweger syndrome. The combination of findings is characteristic and should allow for a rapid and specific diagnosis in the proper clinical setting.

Materials and Methods

The six patients were all determined to have Zellweger syndrome in the neonatal period on the basis of characteristic clinical and laboratory findings. In all cases, the MR images showed abnormalities that confirmed the clinical impression. The hospital records and MR imaging studies of the patients were reviewed retrospectively. Clinical records were scrutinized for findings on physical examination and results of laboratory investigations. Brain MR studies were obtained at ages ranging from 4 to 42 days (mean, 19 days). MR examinations were performed at several different centers and slightly different techniques were used. The examinations consisted of sagittal 3 to 4-mm spin-echo T1-weighted images, axial 4 to 5-mm spin-echo T1-weighted images, and axial 4-mm spin-echo T2-weighted images (dual echo) in all patients. Coronal spin-echo 5-mm T1-weighted images were obtained in four patients and coronal three-dimensional Fourier transform (3DFT) images with gradient spoilers and 1.5-mm partitions were obtained in two patients. Coronal 4-mm fast spin-echo T2-weighted images were obtained in one patient. The MR studies were reviewed for the state of myelination; the presence, extent, and morphologic appearance of cerebral cortical anomalies; the status of the cerebellar cortex, basal nuclei, and brain stem; and the presence or absence of any regions of abnormal signal in the brain parenchyma.

Color photographs from the gross autopsy specimen of one patient were available for review.

Received October 21, 1996; accepted after revision January 15, 1997.

From the Department of Radiology, University of California, San Francisco (A.J.B.), and the Department of Radiology, St Joseph's Hospital and Children's Hospital of Orange County, Orange, Calif (W.W.P.).

Address reprint requests to A. James Barkovich, MD, Department of Radiology, Neuroradiology Section, University of California, San Francisco, 505 Parnassus Ave, L-371, San Francisco, CA 94143.

AJNR 18:1163–1170, Jun 1997 0195-6108/97/1806–1163

Results

Clinical Presentation

All six patients were delivered vaginally at term. One had perinatal depression with low 1 and 5 minute Apgar scores (2/5). The other five patients had craniofacial dysmorphism, profound hypotonia, neonatal seizures, and weak tendon, sucking, and swallowing reflexes, noted on the first day of life. Two of the patients required reintubation because of aspiration related to the impaired swallowing reflex. Head size was within 2 standard deviations (SD) of normal in all six patients. Congenital glaucoma was diagnosed in three of the patients and two had congenital cataracts. Hepatomegaly was present in four patients. Two had contractures at the elbows and feet. Bilateral cubitus valgus was present in one infant. Cardiac abnormalities were present in two patients, including a patent ductus arteriosus and small atrial septal defect in one and a ventricular septal defect in the other.

Laboratory, Electroencephalographic, and Radiologic Findings

Plasma levels of very long chain fatty acids were tested in three patients and were increased with a marked elevation of C24:C22 (range, 1.8 to 2.1; normal, 0.8) and C26:C22 (range, 0.4 to 0.7; normal, 0.01). Analysis of urine in four patients revealed elevated levels of dicarboxylic acids and dihydroxycholestanoic acid. In three of the patients (the only three so tested), cultured fibroblasts showed a decrease in plasmalogen synthesis enzyme and a marked increase in very long chain (greater than 22 carbons) fatty acids.

Electroencephalographic (EEG) results were available in four patients and showed multifocal spikes and diffuse background slowing in all.

Plain radiographs of the patella were obtained in three patients. All showed patellar stippling.

MR Results

All patients had diminished myelination and dysplastic cortex that involved essentially all of the cerebrum; the cortical region affected most dramatically was from the posterior sylvian region upward to the posterior frontal and parietal lobes (Figs 1 and 2). On T1-weighted MR images, diminished high signal intensity was present in the posterior limbs of the internal capsules in two patients and normal high signal was completely absent from the capsules in the other four (Fig 1B). No low signal was present in the cerebral white matter on T2-weighted images in any of the patients; this includes the posterior portions of the posterior limbs of the internal capsules, which exhibit low signal in healthy neonates (Fig 2B). Some high T1 signal and low T2 signal was present in the dorsal brain stem, most likely representing a combination of myelination of the median longitudinal fasciculus and medial lemnisci and normal gray matter signal of the brain stem nuclei (Fig 1C) (1). In addition, low signal intensity was present in the superior cerebellar peduncles (Fig 1C).

The entirety of the cerebral cortex was abnormal in all patients. The nature of the cortical abnormality differed in different parts of the brain and the extent of abnormality differed among patients. In the temporal lobes, the cortex had normal thickness but the gyral pattern was abnormal; in some, the sulci were too shallow and the gyri too few (Fig 1C), while in others the cortex appeared microgyric (Fig 2B). In the perisylvian cortex, the appearance was that of more typical polymicrogyria, with multiple small gyri and irregularity of the cortical–white matter junction (Fig 2B). The anterior portions of the frontal lobes had a microgyric appearance (Figs 1D and 2B and C). In three patients, the perirolandic cortex was thickened and showed an area of white matter intensity, similar to the "cell-sparse" zone seen in classical lissencephaly (2), between a thin outer layer of gray matter and a thinner inner layer of gray matter (Fig 2C and D). In two of these patients, the medial occipital lobes were similarly affected (Fig 2C). The inner surface of the inner layer was slightly irregular. In all three of these patients, an abnormally deep perirolandic sulcus was present bilaterally in the region of the thickened cortex (Fig 2D).

Cysts were present at the caudothalamic notch in all patients. These were best seen on the sagittal T1-weighted images (Fig 2A) and coronal 3DFT gradient-echo images (Fig 1A). The cysts were isointense with cerebrospinal fluid (CSF) on all imaging sequences and were not visible on axial images.

No abnormalities were detected in the brain stem or cerebellum in any of the patients.

An interesting finding was significant T1 shortening in the globi palladi and dorsal mesencephalon, in the absence of normal T1 short-

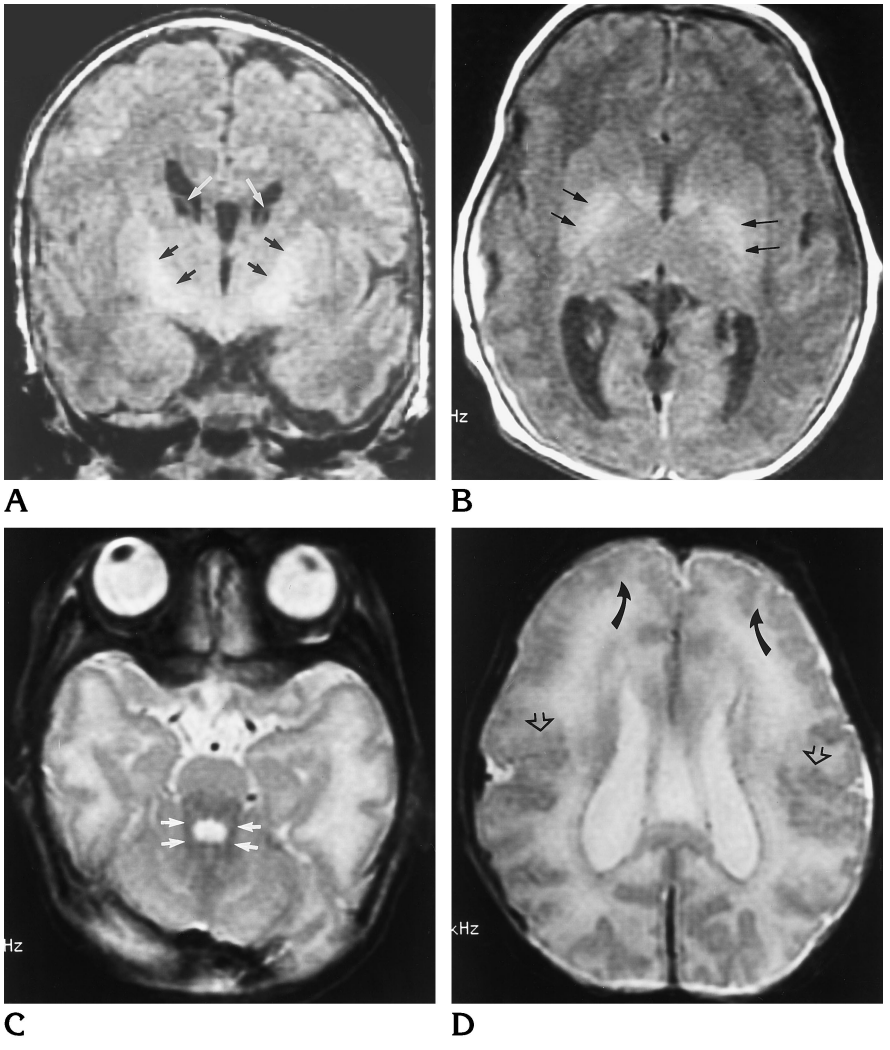

Fig 1. MR findings in a patient with multifocal microgyric cortex and hepatic failure.

A, Coronal 3DFT gradient-echo image shows abnormal hyperintensity (*black arrows*) in the globus pallidus bilaterally and germinolytic cysts (*white arrows*) in the caudothalamic groove bilaterally.

B, Axial spin-echo 500/15 (repetition time/echo time) image shows hyperintensity of the globus pallidus bilaterally (*arrows*) and absence of normal hyperintensity of the posterior limb of the internal capsule. The subacute subdural hematoma is a remnant from vaginal delivery.

C, Axial spin-echo 3000/120 image shows hypointensity in the superior cerebellar peduncles (*arrows*) and dorsal pontine tracts, indicating myelination in those structures. A simplified gyral pattern is present in the temporal lobes.

D, Axial spin-echo 3000/120 image shows an abnormal microgyric pattern in the perirolandic (*open arrows*) and prefrontal (*solid arrows*) regions.

ening in the posterior limb of the internal capsule, in one patient (Fig 1A and B). Review of the chart showed that this patient had hyperbilirubinemia associated with hepatic failure at the time of the MR study.

Autopsy Specimen

Several photographs were available of a single coronal brain slice of the one patient in whom an autopsy was performed. The photographs clearly showed the bilateral germinolytic cysts (Fig 3). The gyral anomalies and hypomyelination were not well seen on the photographs. No microtome specimens or special stains were available for review.

Discussion

Peroxisomes are small cellular organelles that contain multiple compounds that are essential for normal growth and development of the organism. The biochemical functions that take place within peroxisomes include β-oxidation of a specific set of fatty acids and fatty acid derivatives, synthesis of ether-phospholipids and plasmalogens, α-oxidation of phytanic acid, and biosynthesis of cholesterol (3–6). Although peroxisomes were described in 1954 (7), their function and importance in normal development was not discerned for a number of years afterward (8, 9). The function of these organelles and the role of their malfunction in the causation of disease have been substantially clarified over the last two decades (4, 6, 10, 11). Peroxisomal disorders are now classified into three main groups (Table 1). Patients with disorders of group A have abnormal-appearing peroxisomes with a generalized loss of peroxisomal function; the underlying defect is believed to be an inability to import into the per-

Fig 2. Pachygyric and polymicrogyric MR appearance in a single patient.

A, Sagittal spin-echo 600/11 image shows a germinolytic cyst (*curved arrow*) in the caudothalamic groove. Note lack of normal sulcation in frontal lobes (*straight arrows*).

B, Axial spin-echo 3000/120 image shows a paucity of myelin in the posterior limb of the internal capsule. In addition, microgyric cortex (*arrows*) is present in the frontal, temporal, and insular cortices.

C, Axial spin-echo 3000/120 at a slightly higher level than *B* shows macrogyri in the medial right occipital lobe (*open arrow*) and in the perirolandic regions (*solid arrows*). The anterior frontal cortex remains microgyric at this level.

D, Axial spin-echo 3000/120 at a higher level than *C* shows the appearance of two layers of gray matter (*thick solid arrows*) with intervening layer of white matter intensity in the perirolandic and parietal regions. The inner surface of the inner layer of gray matter (*thin solid arrows*) appears irregular in some regions. Large perirolandic infoldings of cortex (*open arrows*) are present bilaterally. Much of the remainder of the cortex appears microgyric.

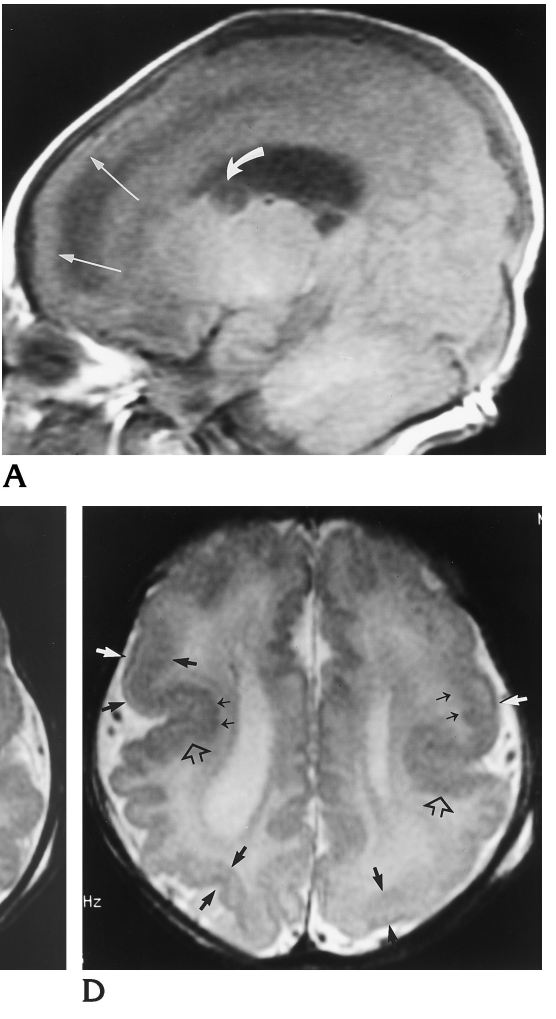

oxisome certain proteins that are synthesized in the cytoplasm (6, 12). Patients with disorders of group B have normal-appearing peroxisomes but loss of multiple peroxisomal functions. Patients classified in group C have normal-appearing peroxisomes and loss of a single peroxisome function (4).

Zellweger syndrome falls into group A, along with neonatal adrenoleukodystrophy, infantile Refsum disease, and, according to some but not all authors, hyperpipecolic acidemia (4, 13). Patients with classic Zellweger syndrome are identified in the nursery by typical craniofacial dysmorphia (high forehead, large anterior fontanel, hypoplastic supraorbital ridges, epicanthal folds, midface hypoplasia), ocular anomalies (cataracts, glaucoma, corneal clouding, pigmentary retinopathy), severe hypotonia, neonatal seizures, and hepatomegaly. All of our patients had some degree of craniofacial dysmorphism; however, ocular anomalies were present in only three and hepatomegaly in four. Affected patients usually survive for less than 1 year; indeed, four of our patients have died and the other two, both of whom are less than 14 months old, are deteriorating.

Neuropathologic examination of the brains of patients with Zellweger syndrome show that the gyri are “too numerous, too small, and too broad” (14). According to Evrard et al (15), the small numerous gyri do not represent true polymicrogyria, but merely too many gyri with a decreased amplitude. All our patients had regions of gyri that were too numerous and too small (Figs 1D and 2B–D). Abnormal deep sulci (“clefts”) have been described in the sylvian (16) and parietal (17) regions. We noted such clefts in four of our patients (Fig 2C and D). Few reports of the MR appearance of the brains of patients with Zellweger syndrome have been published; our Medline search revealed one report in which van der Knaap and Valk (18)

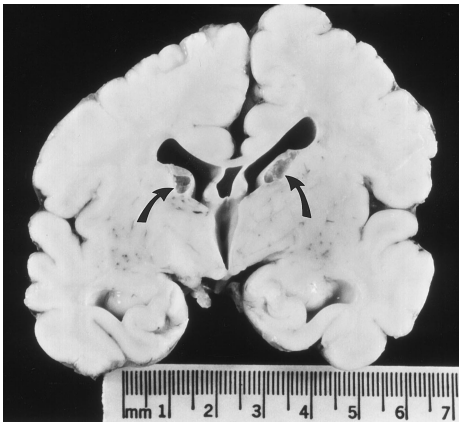

Fig 3. Coronally cut gross autopsy specimen shows the bilateral germinolytic cysts (*arrows*). The sulcal appearance is difficult to determine on this single slice.

Classification of peroxisomal disorders

Group A: Deficiency of peroxisomes with generalized loss of peroxisomal function
1. Cerebrohepatorenal (Zellweger) syndrome
2. Neonatal adronoleukodystrophy
3. Infantile Refsum disease
(4. Hyperpipecolic acidemia)
Group B: Loss of multiple peroxisome functions (peroxisomes present)
1. Rhizomelic chondrodysplasia punctata
2. Zellwegerlike syndrome
Group C: Loss of single peroxisome function (peroxisomes present)
1. X-linked adrenoleukodystrophy and variants
2. Acyl-CoA oxidase deficiency (pseudo-NALD)
3. Bifunctional enzyme deficiency
4. Peroxisomal thiolase deficiency (pseudo-Zellweger)
5. Dihydroxyacetone phosphate acyltransferase deficiency
6. Alkyldihydroxyacetone phosphate synthase deficiency
7. Di- and trihydroxycholestanoic adidemia
8. Glutaryl-CoA oxidase deficiency
9. Hyperoxaluria type I
10. Acatalasemia

describe a single case of Zellweger syndrome in their article on MR imaging of peroxisomal disorders. Their case shows some incomplete frontal sulcation and perirolandic polymicrogyria, similar to that in the patient in Figure 1. This brings up an interesting finding in our six patients with this syndrome: namely, marked variation in the extent and appearance of cortical abnormalities. This variation was seen both within the same patient and across the patient population. Some cortical regions had normal or slightly diminished thickness with an irregular microgyric pattern consisting of multiple shallow sulci separating small gyri; this appearance was seen in the anterior frontal and perisylvian cortex in all patients and in the temporal lobes of some (Figs 1D and 2B–D). In other areas, the cortical thickness appeared normal but the gyri were broad and flat (Fig 1C). In addition, three patients (Fig 2D) had cortical regions that appeared quite similar to that seen in type 1 lissencephaly (19); a thin outer cortical layer was separated from a thicker underlying layer of gray matter by a cell-sparse zone (Fig 2C and D). However, the inner surface of the inner gray matter layer had a slightly irregular contour, in contrast with the smooth contour seen in type 1 lissencephaly. Our findings are supported by the pathologic findings reported by Friede (20), who stated that some cortical areas in Zellweger syndrome are typical of pachygyria and others are typical of polymicrogyria.

The other major neuropathologic finding that has been reported is that of severely abnormal myelination. This appears to be primarily a hypomyelination, in contradistinction to dysmyelination or demyelination (21). It is speculated that the lack of myelination results from the lack of formation of plasmalogens, which are a major component of the normal myelin membrane (4, 21). Another factor may be the abundance of very long chain fatty acids; it is thought that the presence of very long chain fatty acids in membrane phospholipids might destabilize the affected membrane (22), in this case myelin. Impaired cholesterol biosynthesis (another peroxisomal function) may also affect myelin formation. The MR images in our study clearly showed impaired myelination: the T1 and T2 shortening in locations characteristic of early myelination was diminished in the cerebrum of all the patients. One of our patients (Fig 1A and B) did have some T1 shortening in the cerebrum; however, the T1 shortening was in the globi palladi, not the internal capsule. On further investigation, it was found that the patient was hyperbilirubinemic from hepatic dysfunction, another manifestation of Zellweger syndrome. Theoretically, one might be led away from the correct diagnosis by misinterpreting this T1 shortening as myelination. However, because the ventrolateral thalami and the posterior limb of the internal capsule myelinate earlier than the globus pallidus (23), one does not see myelination in the globus pallidus in the absence of myelination in the ventrolateral thalamus and posterior limb of the internal capsule in the neonatal brain. In addition, hypoxic-ischemic injury, which can cause hyperintensity of

the globus pallidus, also causes hyperintensity of the ventrolateral thalamus (24); such hyperintensity was not present in this case. Thus, the most likely cause of the globus pallidus hyperintensity in this case was the known hyperbilirubinerma. It is important to be aware of the possibility of hepatic dysfunction in affected neonates and to interpret the MR study only after acquiring adequate clinical information.

Subependymal germinolytic cysts are believed to result from hemorrhage into and subsequent lysis of the telencephalic subependymal germinal matrix (20). These cysts can occur anywhere along the walls of the lateral ventricles, but are most commonly seen in the region of the ganglionic eminence of the germinal matrix, the last portion of the germinal matrix to involute. The ganglionic eminence is located near the junction of the caudate head and the thalamus, a region known as the caudothalamic notch. The cysts are nonspecific with respect to pathogenesis and have been described in patients with congenital heart disease, congenital or neonatal infection, prenatal hemorrhage, and lactic acidemia, as well as in those with Zellweger syndrome (25–27). Although they are nonspecific, these cysts have a characteristic appearance (Figs 1A, 2A, and 3) and can be a useful finding in patients with suspected Zellweger syndrome, as they are easily detected by transfontanel sonography (25–27) and MR imaging. In contrast, the other, more specific, findings of hypomyelination and cortical malformation can be detected only with MR imaging.

Other reported neuropathologic findings in Zellweger syndrome include abnormal olivary nuclei, cerebellar hypoplasia, and migrational defects of the cerebellar Purkinje cells (13, 14). None of these abnormalities was observed on our MR studies.

The main disorder from which Zellweger syndrome must be differentiated, according to most child neurology texts (13), is neonatal adrenoleukodystrophy (NALD). Although some authors consider Zellweger syndrome to be distinct from NALD, others believe the two disorders are parts of a continuum. Powers (21) and Norman et al (14) point out that Zellweger patients have hypomyelination, whereas NALD patients have demyelination with inflammatory cells and foamy macrophages in the white matter. In addition, the cortical malformations seen in Zellweger patients are described as more common and more severe than those in NALD patients. Kelley et al (28) have proposed criteria to discriminate Zellweger syndrome from NALD, suggesting that NALD patients have adrenal atrophy, cerebral demyelination, systemic infiltration of lipid-laden macrophages, and elevated levels of saturated very long chain fatty acids, whereas Zellweger patients have chondrodysplasia, glomerulocystic kidney disease, central nervous system (CNS) dysmyelination, and accumulation of both saturated and unsaturated very long chain fatty acids. While these are strong arguments, other authors are equally convincing in suggesting that NALD is just a milder phenotype of the same disease (13, 29). Moser (13) points out that patients with Zellweger syndrome, NALD, and infantile Refsum disease (which he also considers part of the same spectrum) can all have the same genotype. This view of a spectrum of phenotypic expression is supported by the observation of Norman et al (14) that the severity of inflammatory changes seen in the cerebral white matter of patients with Zellweger syndrome seems to increase with the duration of survival after birth. Thus, it may be that patients said to have Zellweger syndrome have poor survival because they have severe cortical malformations and consequent epilepsy; because their survival is short, the white matter shows little inflammatory changes. Those patients with lesser cortical malformations presumably survive longer and have more inflammatory changes in the white matter; these patients are considered to have NALD.

Other differential considerations in this group of patients are the peroxisomal bifunctional enzyme defect (BFD) (30), acyl-CoA oxidase deficiency (pseudo-NALD) (31), and peroxisomal thiolase deficiency (pseudo-Zellweger) (32); patients with all these diseases have neonatal courses and many phenotypic manifestations that are similar to those with Zellweger syndrome (4). Congenital muscular dystrophies that are associated with brain malformations (Walker-Warburg syndrome [33, 34], Fukuyama congenital muscular dystrophy [35, 36], Santavuori muscle-eye-brain disease [37–39], and other muscular dystrophies with brain involvement [40, 41]) are also diagnostic considerations from an imaging perspective, as all these disorders have malformations of cortical development associated with abnormal myelination. We were unable to find any published

MR brain images of BFD, pseudo-NALD, or pseudo-Zellweger. However, one would expect BFD to have great neuroradiologic similarity to Zellweger syndrome. Published brain autopsy findings in BFD show hypomyelination and bilateral, symmetric cortical malformations in the perirolandic and sylvian regions. Microscopic examination revealed pachygyria and unlayered polymicrogyria with poor demarcation of the cortex and underlying white matter (42). These findings are similar to those in our cases of Zellweger syndrome. Moreover, these similarities suggest that the peroxisomal bifunctional enzyme is in some way related to the processes of neuronal migration and organization. In contrast to the findings in BFD, autopsy findings in a patient with pseudo-Zellweger syndrome revealed hypomyelination but a normal cerebral cortex (32); most abnormalities were in the cerebellum. Findings on a head computed tomographic (CT) scan of pseudo-NALD were reported to be normal (43).

Most of the congenital muscular dystrophies can be differentiated from Zellweger syndrome clinically, in that most affected patients are not as sick in the neonatal period; do not have the typical Zellweger facies; do not have hepatic, renal, or adrenal dysfunction; and do not have neonatal seizures. The one congenital muscular dystrophy that may be accompanied by profound hypotonia and seizures in the neonatal period is Walker-Warburg syndrome. Patients with this disorder can be differentiated from those with Zellweger syndrome by using MR imaging to detect the many associated CNS anomalies present in Walker-Warburg patients, including hydrocephalus, ocular anomalies (typically, persistent hyperplastic primary vitreous), corpus callosal hypogenesis or agenesis, and lissencephaly involving the entirety of the cerebrum (19). In contrast to those patients with Walker-Warburg syndrome, changes of muscular dystrophy are not present on muscle biopsy specimens of patients with Zellweger syndrome. Finally, the presence of germinolytic cysts has not been demonstrated in Walker-Warburg syndrome and may be a useful feature in establishing an imaging diagnosis.

Although we did not have CT scans or sonograms to compare with the MR studies of our patients, it appears that MR imaging should be the neuroimaging study of choice in the assessment of patients with suspected Zellweger syndrome. MR imaging is the only technique that can show the sometimes subtle cortical malformations and hypomyelination that are crucial in making the diagnosis. Although germinolytic cysts can be detected by sonography and perhaps by CT, they are, by themselves, nonspecific as discussed earlier.

In summary, we have described the MR imaging findings in six patients with cerebrohepatorenal, or Zellweger, syndrome. Although the imaging appearance varies slightly from case to case, the combination of hypomyelination, diffusely abnormal gyration that is most severe in the perisylvian and perirolandic regions, and germinolytic cysts in the caudothalamic groove should allow confident diagnosis of this disorder in the proper clinical setting.

References

1. Martin E, Krassnitzer S, Kaelin P, Boesch C. MR imaging of the brainstem: normal postnatal development. *Neuroradiology* 1991; 33:391–395
2. Barkovich AJ, Koch TK, Carrol CL. The spectrum of lissencephaly: report of ten cases analyzed by magnetic resonance imaging. *Ann Neurol* 1991;30:139–146
3. Vanden Bosch H, Schutgens RBH, Wanders RJA, Tager JM. Biochemistry of peroxisomes. *Ann Rev Biochem* 1992;61:157–197
4. Wanders RJA, Schutgens RBH, Barth PG. Peroxisomal disorders: a review. *J Neuropathol Exp Neurol* 1995;54:726–739
5. Krisans SK. The role of peroxisomes in cholsterol metabolism. *Am J Resp Cell Mol Biol* 1992;7:358–364
6. Lazarow PB. Peroxisome structure, function and biogenesis: human patients and yeast mutants show strikingly similar defects in peroxisome biogenesis. *J Neuropathol Exp Neurol* 1995;54:720–725
7. Rhodin J. Correlation of ultrastructural organization and function in normal and experimentally changed proximal convoluted tubule cells of the mouse kidney. Stockholm, Sweden: Aktiebolaget Godvil; 1954
8. Singh I, Moser AB, Goldfischer S, Moser HW. Lignoceric acid is oxidized in the peroxisomes: implications for the Zellweger cerebrohepatorenal syndrome and adrenoleukodystrophy. *Proc Natl Acad Sci U S A* 1984;81:4203–4207
9. Goldfischer S, Moore CL, Johnson AB, et al. Peroxismoal and mitochnodrial defects in the cerebro-hepato-renal syndrome. *Science* 1973;182:62–64
10. Moser HW, Mihalik SJ, Watkins PA. Adrenoleukodystrophy and other peroxisomal disorders that affect the nervous system, including new observations on L-pipecolic acid oxidase in primates. *Brain Dev* 1989;11:80–90
11. Naidu S, Moser AE, Moser HW. Phenotypic and genotypic variability of generalized peroxisomal disorders. *Pediatr Neurol* 1988; 4:5–12
12. Braverman N, Dodt G, Gould SJ, Valle D. Disorders of peroxisome biogenesis. *Hum Mol Genet* 1995;4:1791–1798
13. Moser HW. Peroxisomal disorders. In: Berg BO, ed. *Principles of Child Neurology*. New York, NY: McGraw-Hill; 1996:1233–1248
14. Norman MG, McGillivray BC, Kalousek DK, Hill A, Poskitt KJ. Congenital malformations of the brain: pathologic, embryologic, clinical, radiologic and genetic aspects. Oxford, England: Oxford University Press; 1995:223–307

15. Evrard P, Caviness VSJ, Prats-Vinas J, Lyon G. The mechanism of arrest of neuronal migration in the Zellweger malformation: an hypothesis based upon cytoarchitectonic analysis. *Acta Neuropathol* 1978;41:109–117
16. Volpe JJ, Adams RD. Cerebro-hepato-renal syndrome of Zellweger: an inherited disorder of neuronal migration. *Acta Neuropathol* 1972;20:175–198
17. deLeón GA, Grover WD, Huff DS, Morinigo-Mestre G, Punnett HH, Kistermacher ML. Globoid cells, glial nodules, and peculiar fibrillary changes in the cerebro-hepato-renal syndrome of Zellweger. *Ann Neurol* 1977;2:473–484
18. van der Knaap MS, Valk J. The MR spectrum of peroxisomal disorders. *Neuroradiology* 1991;33:30–37
19. Barkovich AJ, Gressens P, Evrard P. Formation, maturation, and disorders of brain neocortex. *AJNR Am J Neuroradiol* 1992;13: 423–446
20. Friede RL. *Developmental Neuropathology*. 2nd ed. Berlin, Germany: Springer; 1989
21. Powers JM. The pathology of peroxisomal disorders with pathogenetic considerations. *J Neuropathol Exp Neurol* 1995;54:710–719
22. van der Knaap MS, Valk J. Myelin and white matter. In: van der Knaap MS, Valk J, eds. *Magnetic Resonance of Myelin, Myelination, and Myelin Disorders*. 2nd ed. Berlin, Germany: Springer; 1995:1–17
23. Hasegawa M, Houdou S, Mito T, Takashima S, Asanuma K, Ohno T. Development of myelination in the human fetal and infant cerebrum: a myelin basic protein imminohistochemical study. *Brain Dev* 1992;14:1–6
24. Barkovich AJ, Westmark KD, Ferriero D, Sola A, Partridge C. Perinatal asphyxia: MR findings in the first 10 days. *AJNR Am J Neuroradiol* 1995;16:427–438
25. Mito T, Ando Y, Takeshite K, et al. Ultrasonographical and morphological examination of subependymal cystic lesions in maturely born infants. *Neuropediatrics* 1989;20:211–214
26. Russel IMB, van Sonderen L, van Straaten HLM, Barth PG. Subependymal germinolytic cysts in Zellweger syndrome. *Pediatr Radiol* 1995;25:254–255
27. Shackelford GD, Fulling KH, Glasier CM. Cysts of the subependymal germinal matrix: sonographic demonstration with pathologic correlation. *Radiology* 1983;149:171–175
28. Kelley RI, Datta NS, Dobyns WB, et al. Neonatal adrenoleukodystrophy: new cases, biochemical studies, and differentiation from Zellweger and related peroxisomal polydystrophy syndromes. *Am J Med Genet* 1986;23:869–901
29. van der Knaap MS, Valk J. Zellweger cerebrohepatorenal syndrome, neonatal adrenolekukdystrophy, and infantile Refsum disease. In: van der Knaap MS, Valk J, eds. *Magnetic Resonance of Myelin, Myelination, and Myelin Disorders. 2nd ed*. Berlin, Germany: Springer; 1995:110–120
30. Watkins PA, Chen WW, Harris CJ, et al. Peroxisomal bifunctional enzyme deficiency. *J Clin Invest* 1989;83:771–777
31. Poll-The BT, Roels F, Ogier H, et al. A new peroxisomal disorder with enlarged peroxisomes and a specific deficiency of acyl-CoA oxidase (pseudo-neonatal adrenoleukodystrophy). *Am J Hum Genet* 1988;41:422–434
32. Goldfischer S, Collins J, Rapin I, et al. Pseudo-Zellweger syndrome: deficiencies in several peroxisomal oxidative activities. *J Pediatr* 1986;108:25–32
33. Williams RS, Swisher CN, Jennings M, Ambler M, Caviness VSJ. Cerebro-ocular dysgenesis (Walker-Warburg syndrome): neuropathologic and etiologic analysis. *Neurology* 1984;34:1531–1541
34. Dobyns WB, Kirkpatrick JB, Hittner HM, Roberts RM, Kretzer FL. Syndromes with lissencephaly. 2: Walker-Warburg and cerebral occular muscular syndromes and a new syndrome with type 2 lissencephaly. *Am J Med Genet* 1985;22:157–195
35. Aida N, Tamagawa K, Takada K, et al. Brain MR in Fukuyama congenital muscular dystrophy. *AJNR Am J Neuroradiol* 1996; 17:605–614
36. Fukuyama Y, Kawazura M, Haruna H. A peculiar form of congenital muscular dystrophy: report of fifteen cases. *Paediatr Univers (Tokyo)* 1960;4:5–8
37. Santavuori P, Leisti J, Kruus S. Muscle, eye and brain disease: a new syndrome. *Neuropädiatrie (Suppl)* 1977;8:553–558
38. Santavuori P, Somer H, Sainio K, et al. Muscle-eye-brain disease. *Brain Dev* 1989;11:147–153
39. Valanne L, Pihko H, Katevuo K, Karttunen P, Somer H, Santavuori P. MRI of the brain in muscle-eye-brain (MEB) disease. *Neuroradiology* 1994;36:473–476
40. Trevisan CP, Martinello F, Ferruzza E, et al. Divergence of central nervous system involvement in 2 Italian sisters with congenital muscular dystrophy: a clinical and neuroradiological follow-up. *Eur Neurol* 1995;35:230–235
41. Pini A, Merlini L, Tomé FMS, Chevallay M, Gobbi G. Merosin-negative congenital muscular dystrophy, occipital epilepsy with periodic spasms and focal cortical dysplasia: report of three Italian cases in two families. *Brain Dev* 1996;18:316–322
42. Kaufmann WE, Theda C, Naidu S, Watkins PA, Moser AB, Moser HW. Neuronal migration abnormality in peroxisomal bifunctional enzyme defect. *Ann Neurol* 1996;39:268–271
43. Kyllerman M, Bloomstrand S, Mansson JE, Conradi N, Hinmarsh T. Central nervous system malformations and white matter changes in pseudo-neonatal adrenoleukodystrophy. *Neuropediatrics* 1989;21:199–201